Mitochondrial Physiology Network 06.03(14):1-8 (2015)
A: http://wiki.oroboros.at/index.php/MiPNet06.03_POS-Calibration-SOP

Version 14: 2015-08-31

Polarographic oxygen sensors: calibration, accuracy and quality control SOP

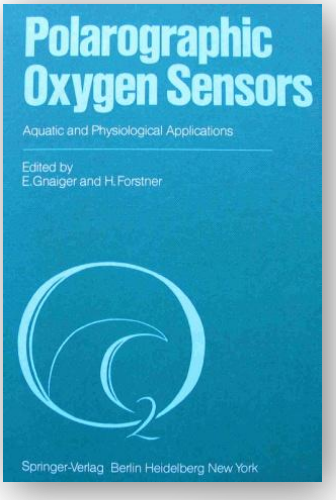

Gnaiger E

OROBOROS INSTRUMENTS
O2k high-resolution respirometry
Schöpfstr 18, A-6020 Innsbruck, Austria
erich.gnaiger@oroboros.at; www.oroboros.at
Medical University of Innsbruck
D. Swarovski Research Laboratory, A-6020 Innsbruck, Austria

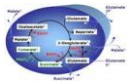

Section **Page**

Summary: High-resolution respirometry (HRR; OROBOROS Oxygraph-2k, O2k) critically depends on maintenance (MiPNet19.18B) and accurate calibration of the polarographic oxygen sensors (**OroboPOS**, POS).

Standard operating procedures (O2k-SOP) are described. (1) Storing and cleaning the O2k-Chambers: clean and ready-to-use O2k-Chambers are a requirement for rapid calibrations and saving time (MiPNet19.03). (2) Quality control for evaluation of proper POS function (O_2 sensor test). (3) Accurate POS calibration (MiPNet19.18D): A POS responds to partial oxygen pressure, p_{O2}. Expressing the signal in terms of p_{O2} has several advantages, but respiration is expressed in molar units related to biochemical stoichiometries. Conversion of oxygen partial pressure to oxygen concentration, c_{O2}, is based on accurate information on barometric pressure (measured electronically) and oxygen solubilities in experimental media. The oxygen solubility of mitochondrial respiration medium MiR06 relative to pure water (oxygen solubility factor, F_M) is 0.92, accurately determined (for MiR05 = MiR06 without catalase; MiPNet14.13) at 37 °C and 30 °C. At air saturation at standard barometric pressure (100 kPa) and 37 °C, the p_{O2} is 19.63 kPa, and the c_{O2} is 190.7 µM in MiR06. Absolute errors >10% are common but cannot be accepted in HRR.

1. Polarographic oxygen sensor

Each O2k-chamber is equipped with a polarographic oxygen sensor (OroboPOS, POS). The polarographic oxygen sensor is developed for optimum function of the O2k. The signal is linear in the extended range of partial oxygen pressure of 20 kPa (and up to pure oxygen: 100 kPa) to zero. Thus POS are superior to optical sensors.

The OroboPOS requires minimum service interventions, operates at a high sensitivity and stability for periods of >3 months without change of the membrane at minimum running costs (MiPNet18.10).

Oxygen diffuses from the sample to the cathode surface through (*1*) an unstirred layer of the sample at the outer membrane surface, (*2*) the membrane and (*3*) the electrolyte layer (Fig. 1). To minimize the unstirred layer of the sample, a high and constant stirring of the sample medium is required. At the cathode the oxygen pressure is effectively held at zero. Under steady-state conditions, the oxygen flux to the cathode depends on the external oxygen pressure, and the electrochemical reduction of oxygen yields an oxygen-dependent consumption of oxygen by the POS which is converted into an electrical signal.

The Clark-type oxygen sensor produces its electrical signal by consuming the oxygen which diffuses across the oxygen-permeable membrane to the cathode (Fig. 1). The cathode and anode reactions are,

$$O_2 + 2\ H_2O + 4\ e^- \rightarrow 4\ OH^-$$
$$4\ Ag \rightarrow 4\ Ag^+ + 4\ e^-$$

At air saturation, the signal of the POS is c. 2 µA. From the stoichiometry (above) and Faraday's law (2.591 pmol $O_2 \cdot s^{-1} \cdot \mu A^{-1}$), oxygen consumption by the POS at air saturation in a 2 cm^3 chamber is theoretically 2.6 $pmol \cdot s^{-1} \cdot cm^{-3}$), in direct agreement with experiment (MiPNet14.06).

A

1.1. Cathode

A gold cathode is generally superior to platinum. The sensitivity of polarographic oxygen sensors is a function of cathode area, and long-term stability increases with a high electrolyte volume and a high ratio of anode to cathode area. The signal to noise ratio increases and the relative signal drift at zero oxygen decreases with cathode area. Therefore, the OROBoPOS has a relatively large cathode area (2 mm diameter), yielding a high sensitivity owing to a stable zero current. Signal noise decreases with decreasing oxygen to less than ±0.003 kPa (recorded near zero oxygen over 100 data points and 1 s intervals) which is of particular advantage for measurements at physiological intracellular oxygen levels.

1.2. Anode

The silver-silver chloride anode has a large area compared to the cathode. The anode may become dark grey-black and is periodically cleaned by treatment with ammonia. Regeneration is possible by a service provided by OROBOROS INSTRUMENTS.

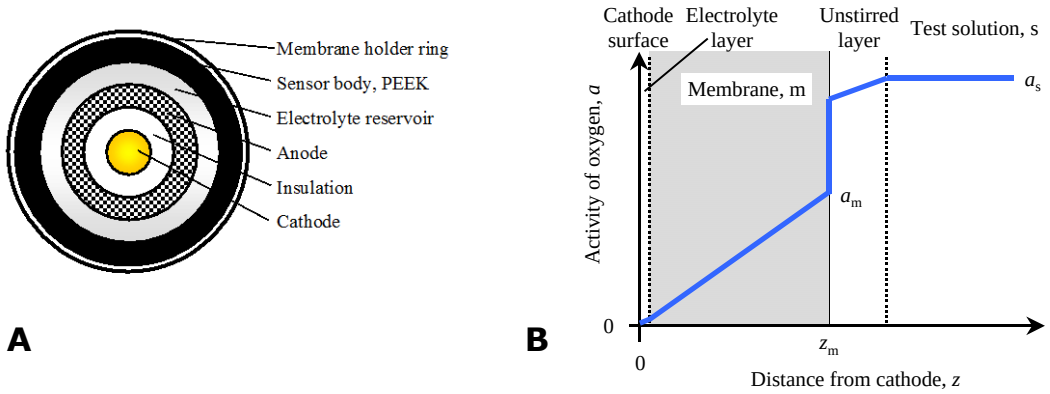

Figure 1. The polarographic oxygen sensor (A) consists of a gold cathode and a silver-silver chloride anode, connected by a KCl electrolyte enclosed by an oxygen-permeable membrane. Oxygen diffusion profile (B) at the polarographic oxygen sensor under steady-state conditions in a stirred test solution.

1.3. Electrolyte

KCl solution (1 mol.dm^{-3}; 74.56 g potassium chloride per liter distilled water). Dissolve 1.49 g KCl in distilled water to yield a total volume of 20 ml. A high quality of deionised or distilled H_2O is critically important. Before filling the electrolyte into the receptacle of the POS, warm it to c. 40 °C to avoid formation of gas bubbles in the electrolyte reservoir of the POS, which is particularly important after storage at 4 °C.

An alkaline electrolyte with KOH did not improve stability of the signal, had no positive effect on the long-term behaviour of the time constant and is less convenient for handling. For these reasons, we do not use a KOH electrolyte.

For a H_2S insensitive mode of operation at high sulfide concentrations, a special electrolyte should be freshly prepared:

Equilibrate distilled water with nitrogen gas. Dissolve 100 g $K_2S{\cdot}9\ H_2O$ in 1 liter distilled water. The dissolution requires a long time with automatic stirring. Filter the black precipitate and store in the dark never longer than 6 weeks. The polarizing voltage must be changed from 800 mV to 100 mV.

1.4. Membrane

At a given oxygen concentration in the test solution, the signal of a POS depends on the properties of the membrane, increasing with diffusion coefficient and oxygen solubility (the product of which is the permeability coefficient), and decreasing with membrane thickness. While a high signal is desirable in terms of a high electronic signal to noise ratio, and a low membrane thickness and high diffusion coefficient increase the time resolution, these advantages are offset by a high background oxygen consumption in the respirometer chamber, an increased sensitivity to the stirring of the sample, and a shortened lifetime of the anode and electrolyte. Therefore, the choice of the membrane requires optimization according to specific requirements. OroboPOS-membranes (FEP, 25 µm thickness) are used for high-resolution respirometry. Application of a new membrane is simplified by the OroboPOS-Service Kit.

2. Calibration and quality control (O2k-SOP)

1. Switch on the O2k. Edit O2k-settings in DatLab and connect. Clean the O2k-Chambers (MiPNet19.03).
2. Rise the temperature of experimental medium slightly above experimental before adding 2.1-2.5 ml medium into each O2k-Chamber, to avoid the formation of gas bubbles and minimize the temperature disturbance.
3. With the stirrer on (typically 750 rpm), insert the stopper fully, check that no air bubbles are contained in the volume-calibrated chamber.
4. Siphon off excess medium from the top of the stopper.
5. Lift the stopper to the stopper spacer position.

» MiPNet19.18D O2k-Calibration.

1. About 20 min are required for approximate air equilibration after temperature equilibration of the incubation medium (Fig. 2; time scale is 1 h).

   Quality control **a**: The raw signal (blue plot; 1 V = 1 µA at a gain setting of 1) should be close to 1 to 3 V at 25 to 37 °C at sea level up to 1000 m (p_b 101 to 90 kPa). It should be very close to the raw signal obtained at a previous calibration under identical experimental

A

conditions. See O2-Calibration window (**a'**). At gain setting of 2 the raw signal [V] is multiplied by 2.

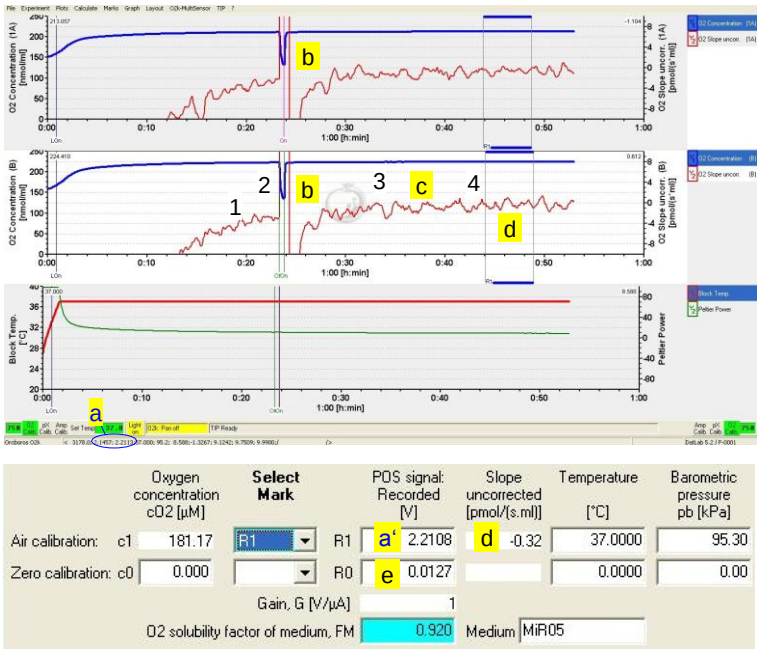

Figure 2. Quality control of POS performance.

2. Even before final equilibration, perform a stirrer test [F9], switching both stirrers automatically off for 30 s.

Quality control **b**: Upon automatic re-start of the stirrer (On), the increase of the oxygen signal should be rapid and monoexponential (Fig. 3; 30 min time scale).

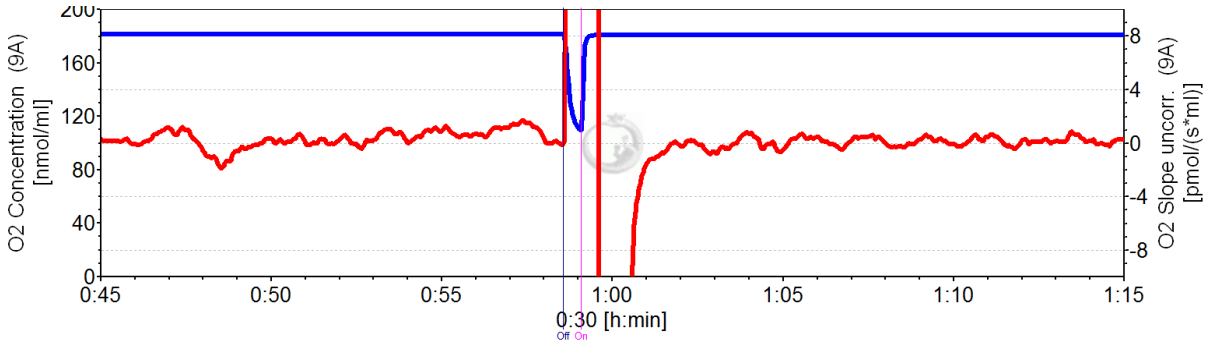

Figure 3. Stirrer test for quality control (standard 30 s) with 30 min time scale displayed with Graph Layout "02-Background experiment" (MiR05; 37 °C; data recording interval: 2 s; slope smooting: 40 data points). 2014-02-19 P9-01.DLD

3. Within 40 min, the oxygen signals should be stable with O2 slope (uncorrected) close to zero.

Quality control **c**: Signal noise should be low, reflected in a noise of the O2 slope (red plot) within ±2 (±4 is acceptable) pmol·s^{-1}·ml^{-1} at a data recording interval of 2 s and 40 data points selected for calculation of the slope (Fig. 2).

4. Set a mark on the oxygen signal (R1) and click on O2 Calib. to open the DatLab O_2 calibration window.

Quality control **d**: The slope uncorrected should be within ±1 pmol·s^{-1}·ml^{-1} averaged across the section of the experiment marked as R1 for air calibration.

5. Continue with an instrumental O_2 background test (MiPNet14.06) and perform a zero oxygen calibration.

Quality control **e**: The zero signal at mark R0 for zero calibration should be <2% of R1 (stable at <5% is acceptable).

3. Zero oxygen calibration

3.1. Zero calibration with instrumental O_2 background test: TIP2k

O2k-SOP: » MiPNet14.06 InstrumentalBackground

3.2. Zero calibration: manual titration of dithionite (O2k-SOP)

1. Prepare "zero solution" by dissolving c. 20 mg sodium hydrosulfite (Na-dithionite, $Na_2S_2O_4$; OroboPOS-Service Kit) or two tips of a spatula in 0.5 ml of water. Mix in a small vial with minimum gas space. Use fresh. Dithionite may not work after prolonged storage.
2. With the stirrer on, insert the stopper fully
3. Inject immediately c. 20 µl into the closed O2k-Chamber. A 50 µl Hamilton syringe is recommended.
4. Oxygen depletion is very rapid, zero oxygen is reached within a few minutes, but a few more minutes may be required until a stable "zero" signal is obtained, R_0 [V].
5. Inject again 10 µl zero solution. Repeat as long as the signal responds by a further decline. Siphon off excess medium from the stopper.
6. The zero signal stabilizes quickly (<±0.2 pmol·s^{-1}·ml^{-1}; compare Fig. 3).
7. Set a mark over the stable "zero" signal (R_0), to complete the two-point oxygen calibration [F5]. Select Mark R1 and Mark R0 for R_1 and R_0.

go Bioblast » MiPNet19.18D O2k-Calibration.

3.3. Zero calibration: mitochondrial respiration

Due to the high oxygen affinity of isolated mitochondria, intact cells and tissue homogenate, residual traces of oxygen are insignificant after respiratory oxygen depletion. Use your experimental sample for such zero oxygen calibration. Alternatively, prepare a stock of bakers yeast, with 200 mg dry yeast in 2 ml physiological salt solution. Stirr heavily to obtain a homogenous suspension of yeast cells and add 50 µl yeast suspension into the 2 ml chamber through the cannula of the stopper, using a Hamilton syringe.

More details: Gnaiger et al (1995), Gnaiger (2001).

A

4. O2-Calibration-List: quality control

OROBOROS FileFinder: Click on the icon in the section "O2k-Manual". Go to Chapter 'Oxygen calibration by DatLab' and move to the right to open the Excel file "O2k-Calibration-List". Save a copy of this Excel Template and paste the calibration parameters into new lines sequentially for chamber (A) and (B), thus generating a data base for quality control of instrumental calibration.

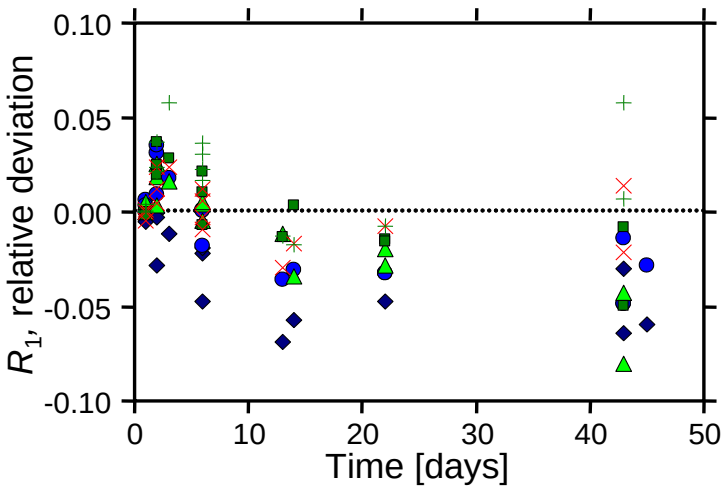

Figure 4. Stability of the signals of six OroboPOS at air calibration, R1, over a period of >1 month at constant temperature (25 °C). Membranes were not exchanged and the sensors were left mounted to the O2k-Chambers, which were filled with 70% ethanol during storage, and with mitochondrial respiration medium during calibrations (from Gnaiger 2008).

Trends over time can thus be evaluated (Fig. 4; Gnaiger 2008), and possible irregularities of sensor performance are quickly recognized for intervention (MiPNet19.18B POS-Service).

5. O_2-sensor test: when?

An O2-sensor test should be performed:

1. After switching on the O2k, every day: air calibration and stirrer test.
2. Zero oxygen calibration: from time to time over weeks; bracketing zero oxygen calibrations when working at low oxygen.
3. After application of a new membrane and O_2-sensor service: in some cases, the signal of the OroboPOS improves (higher signal stability, less noise, shorter response time), when the O2k remains switched on over night (O2k-Chambers filled with 70% EtOH).
4. For quality control of instrumental performance.
5. During troubleshooting procedures, when switching components between the two chambers, a quick sensor

test is performed after each step (stirrer test, sensor signal).

6. References

Gnaiger E (2001) Bioenergetics at low oxygen: dependence of respiration and phosphorylation on oxygen and adenosine diphosphate supply. Respir Physiol 128:277-97. »

Gnaiger E (2008) Polarographic oxygen sensors, the oxygraph and high-resolution respirometry to assess mitochondrial function. In: Mitochondrial Dysfunction in Drug-Induced Toxicity (Dykens JA, Will Y, eds) John Wiley:327-52. »

Gnaiger E, Forstner H, eds (1983) Polarographic Oxygen Sensors. Aquatic and Physiological Applications. Springer, Berlin, Heidelberg, New York:370 pp. »

Gnaiger E, Steinlechner-Maran R, Méndez G, Eberl T, Margreiter R (1995) Control of mitochondrial and cellular respiration by oxygen. J Bioenerg Biomembr 27:583-96. »

Full version

» http://wiki.oroboros.at/index.php/MiPNet06.03_POS-Calibration-SOP

Supplement A: Calibration of time constant for signal correction

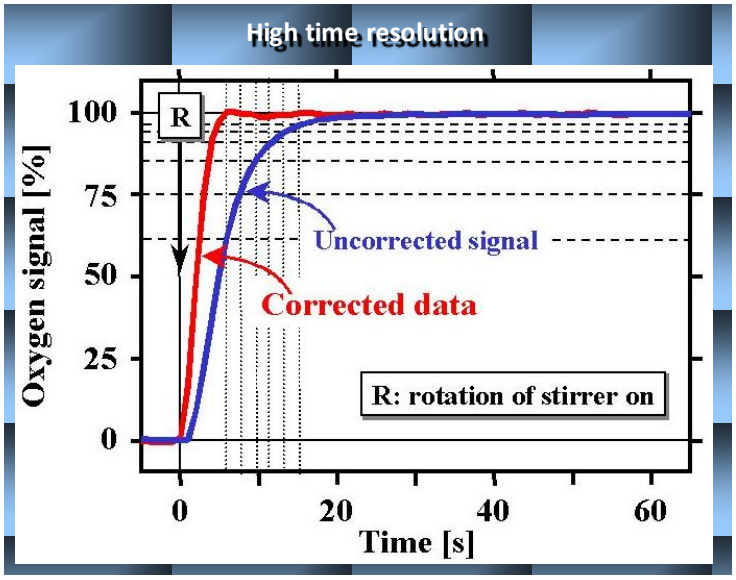

Figure 5. Sensors respond with a time delay to rapid changes of oxygen (uncorrected signal). A step change is simply achieved by switching the stirrer off at air saturation, allowing for a local depletion of oxygen at the cathode, followed by switching the stirrer on. The oxygen signal is expressed in % of the total step change. Is the oxygen sensor sufficiently fast for kinetic studies? DatLab yields the answer, gives the exponential time constant (3 s in the present example) and displays the time-corrected data (modified after Gnaiger 2001).

Correction for the time response by using an accurate time constant is essential for high-resolution analysis of kinetic studies, such as ADP pulse titrations and oxygen kinetics involving rapid transitions to anoxia (Gnaiger 2001).

The signal of polarographic oxygen sensors responds with a time delay to rapid changes in the partial pressure of oxygen in the medium (Fig. 5). This convolution of the signal is due to the separation of the oxygen sensor from the experimental medium by a membrane and an electrolyte layer. Consequently, the signal at the cathode responds to a change in oxygen only after oxygen diffusion has taken place through the membrane to the cathode (Fig. 1B). The time response to changes of p_{O_2} depends mainly on the thickness of the sensor membrane (z_m), the oxygen permeability of the membrane, temperature, and the unstirred boundary layer of the experimental solution (Fig. 1B).

The response time of the oxygen sensor is characterized by an exponential time constant, τ. Knowledge of τ is crucial both for quality control of the POS and for the time correction of O2k recordings in high-resolution respirometry, particularly in kinetic studies. A fast response of the sensor is indicative of a high quality of sensor maintenance. Prolonged use or storage of the sensor without anode cleaning may increase the response time of the sensor. Such a sensor may be used only if the signal is stable and a high time resolution is not required.

τ can be experimentally determined by pulse-titration of anoxic into air-saturated medium or by a stirrer test, i.e. turning the stirrer off and on (Fig. 6). Both methods yield identical results. The response is fitted to an exponential function which yields the value of τ [s].

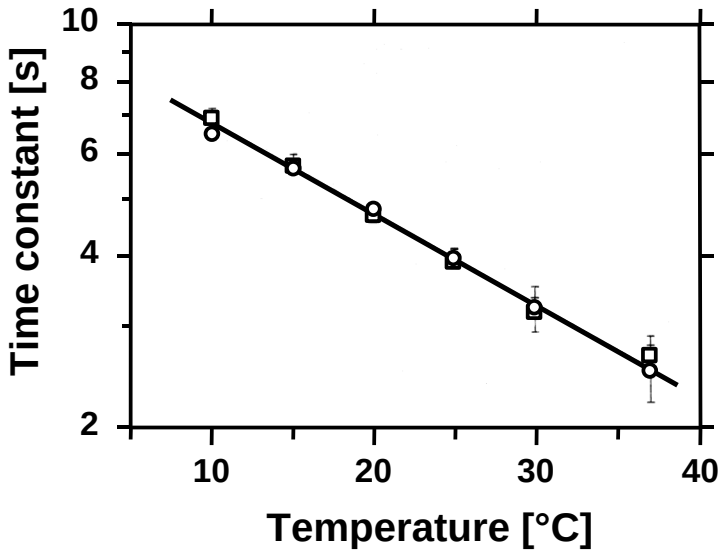

Figure 6. Effect of temperature on the time constant τ. The temperature was varied between 10 and 37 °C, and the time constants of both sensors (chamber A and B in the same Oxygraph) were determined by the titration method. Stirring speed 300 rpm; chamber volume 2 cm³; titration volume 200-250 mm³. Each value represents the mean ± SD of 5-6 measurements (from Gnaiger 2001).

τ depends on experimental temperature, with a Q_{10} of c. 0.69 (Fig. 6). As expected for a diffusion-controlled process, the time constant τ strongly depends on the experimental temperature. A semilogarithmic plot of time constant τ vs. temperature results in a straight line (Fig. 6), indicating a 31% decrease in τ for a 10 °C increase in temperature.

Stirring speed influences τ theoretically only when (1) mixing is slow of the injected (anoxic) solution with the (air-saturated) oxygraph medium (i.e., if the time constant of the mixing process is in the same range or higher than the time constant of the oxygen sensor), or when (2) unstirred layers (Fig. 1B) play a significant role in oxygen diffusion limitation to the cathode. τ is virtually constant between 100 and 700 rpm in anoxic injection experiments, indicating that complete mixing is achieved within a few seconds. A 5% increase of τ between 700 and 100 rpm is consistent with the corresponding 5% decrease of the oxygen signal recorded in air-saturated water. This points to more pronounced unstirred layer effects at lower stirring speeds and, at the same time, excludes a significant contribution of the mixing process to τ. Similarly, an increase in viscosity associated with the addition of 10% dextran to the experimental medium does not significantly affect the time constant.

More details: Gnaiger (2001)

Supplement B: O2 calibration window in DatLab

Figure 7. Upon Show details [F5] (MiPNet19.01D) oxygen calibration parameters are displayed as calculated by DatLab.

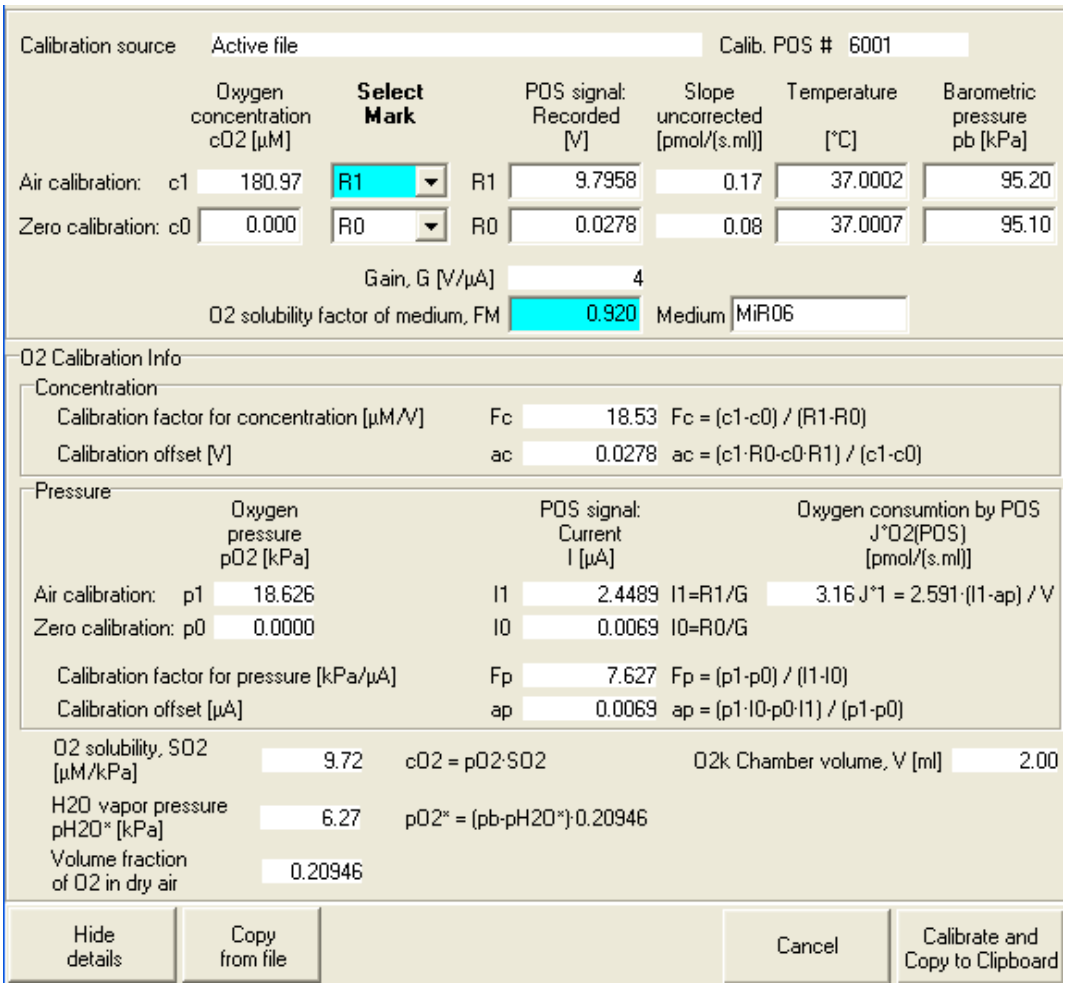

↱**Concentration**: Parameters are displayed for conversion of the raw signal to concentration.

Calibration factor for concentration, F_c [µm/V]: This is the multiplication factor, F_c, calculated to convert the recorded voltage (corrected for the zero signal) into oxygen concentration (Eq. 2).

Calibration offset, a_c [V]: This is the POS zero signal at zero oxygen concentration, which is subtracted from the voltage before multiplication with the calibration factor (Eq. 3).

↱**Pressure**: Parameters are displayed for conversion of the POS signal current to partial oxygen pressure. These are the fundamental parameters for evaluation of signal stability over periods of several months, since the POS responds to partial pressure in the medium rather than concentration.

p_1 [kPa], p_{O_2}: At air saturation, $p_{O_2}^*$, a function of temperature and barometric pressure.

p_0 [kPa]: Usually zero oxygen concentration, or any other p_{O_2} at the second calibration point, p_0.

$I_1 = R_1/G$ [µA]: POS signal as a current, at air saturation (Eq. 4).

$I_0 = R_0/G$ [µA]: POS signal as a current, at zero oxygen concentration, or any other other p_{O_2} at the second calibration point (Eq. 4).

Oxygen consumption by POS, $J°_{O2,POS}$ [pmol·s^{-1}·ml^{-1}]: Theoretical oxygen consumption of the oxygen sensor at air saturation under experimental conditions (Eq. 9).

Calibration factor for oxygen pressure, F_p [kPa/µA]: This is the multiplication factor, F_p, calculated to convert the current of the POS (corrected for the zero current) into oxygen partial pressure (Eq. 6).

Calibration offset, a_p [µA]: This is the POS zero current, at zero oxygen pressure, which is subtracted from the current before multiplication with the calibration factor (Eq. 5).

O_2 solubility [µmol O_2·dm^{-3}·kPa^{-1}]: $S_{O_2} = c_{O_2} \cdot p_{O_2}^{-1}$, a function of temperature and oxygen solubility factor of the medium (Eq. 8).

H_2O vapor pressure [kPa]: $p_{H_2O}^*$, a function of temperature, is subtracted from the barometric pressure, p_b.

Volume fraction of oxygen in dry air: 0.20946, when multiplied with the pressure (p_b - $p_{H_2O}^*$), it yields the partial oxygen pressure.

Gain, G [V/µA]: The gain setting (1, 2, 4 or 8 V/µA) for current to voltage conversion.

O2k chamber volume, V [ml]: The effective aqueous volume of the closed O2k-Chamber.

Supplement C: Equations for oxygen calibration

C1. Oxygen concentration and recorded signal

The recorded oxygen signal, R_t, at experimental time t, is calibrated in terms of oxygen concentration at time t, $c_{O_2}(t)$,

$$c_{O_2}(t) = (R_t - a_c) \cdot F_c \qquad (1)$$

where F_c is the calibration factor based on concentration (Eq. 2),

$$F_c = \frac{c_1 - c_0}{R_1 - R_0} \quad (2)$$

and a_c is the POS signal at zero oxygen concentration,

$$a_c = \frac{c_1 \cdot R_0 - c_0 \cdot R_1}{c_1 - c_0} \quad (3)$$

$c_1 = c_{O_2}^*$ is the oxygen concentration at equilibrium with air. Typically, R_1 and R_0 are the calibration recordings at air saturation and zero oxygen (if c_0 = 0 µM, then $a_c = R_0$.

C2. Oxygen pressure and POS current

In the more general case, the oxygen sensor responds to partial oxygen pressure, and a linear oxygen calibration can be performed at any two calibration pressures of oxygen, p_1 and p_0. The corresponding oxygen signals in terms of current [µA] are I_1 and I_0. A sensor current of 1 µA yields a raw signal of 1 V at a gain setting of 1 V/µA. G is 2 or 4 V/µA in most O2k applications, and can be changed in the O2k Setup window [F7] to 1, 2, 4 or 8 V/µA. The sensor current, I_t, at any time t, therefore, is related to the recorded signal, R_t [V], according to the gain setting,

$$I_t = R_t/G \quad (4)$$

The zero current or offset, a [µA], is

$$a = \frac{p_1 \cdot I_0 - p_0 \cdot I_1}{p_1 - p_0} \quad (5)$$

If the calibration point p_0 is chosen at zero oxygen concentration, then $a = I_0$. The corresponding calibration factor, related to partial pressure and current, is F_p [kPa/µA],

$$F_p = \frac{p_1 - p_0}{I_1 - I_0} \quad (6)$$

After calibration, comparable to Eq.(1), the partial oxygen pressure, $p_{O_2}(t)$, can be calculated from the POS signal current,

$$p_{O_2}(t) = (I_t - a) \cdot F_p \quad (7)$$

C3. Oxygen concentration and oxygen pressure

The oxygen partial pressure is related to the oxygen concentration, $c_{O_2}(t)$ [µM=nmol/ml], by the oxygen solubility, S_{O2} [µM/kPA], which is calculated by DatLab on the basis of experimental temperature and the oxygen solubility factor of the experimental medium, F_M.

$$c_{O_2}(t) = p_{O_2}(t) \cdot S_{O_2} \quad (8)$$

C4. Oxygen signal and background oxygen consumption

The oxygen-related POS current, I_t-a [µA] (Eq. 7), results from the steady-state oxygen diffusion from the medium across the membrane and oxygen consumption at the cathode of the POS. Based on the stoichiometry of 4 electrons per molecule O_2 reduced at the cathode and the Faraday constant (96,485 C/mol), oxygen consumption is expected at 2.591 pmol $O_2 \cdot s^{-1} \cdot \mu A^{-1}$. The oxygen consumption by the POS, per volume of the O2k chamber, V [ml], is $J°_{O_2,POS}$ [pmol·s^{-1}·ml^{-1}], calculated as

$$J°_{O_2,POS} = 2.591 \cdot (I_t - a_p) / V \quad (9)$$

When the O2k-chamber is closed after equilibration at air saturation, the measured instrumental background oxygen consumption, $J°_{O_2}$, can be compared with this theoretical value. Considering the POS signal at gain 2 and 37 °C to be around 4 V (at gain 4: around 8 V), then $I_t - a$ is about 2 µA (Eq. 4). At a volume of 2 ml, therefore, the expected instrumental O_2 background at air saturation is 2.6 pmol $O_2 \cdot s^{-1} \cdot ml^{-1}$ (Eq. 9; MiPNet14.06).

Supplement D: O_2 solubility and concentration at air saturation

D1. Oxygen pressure and concentration

It is practical to calculate the saturation concentration for pure water, which then is corrected by the solubility factor of the medium, F_M, to account for the reduced O_2 solubility in salt media. Owing to the salting-out effect, F_M must be <1.0 in salt media used for respiratory studies of mitochondria, cells and tissues.

F_M is typically near 0.9 for Oxygraph media (0.92 for MiR06 and MiR05; MiPNet14.13). Several oxygen solubilities reported in the literature must be critized on the basis of physicochemical considerations.

Water in equilibrium with air contains an oxygen concentration proportional to the oxygen solubility and the partial oxygen pressure of air. In the gas-liquid boundary, air is saturated with water vapor at the partial pressure of $p_{H_2O}^*$. The water vapor pressure is subtracted from the total barometric pressure, p_b, to obtain the partial pressure of dry air, p_b-$p_{H_2O}^*$. The volume fraction of dry air is constant at Φ_{O_2} = 0.20946. Therefore, the partial oxygen pressure at air saturation is, for any temperature and barometric pressure,

$$p_{O_2}^* = (p_b - p_{H_2O}^*) \cdot 0.20946 \quad (10)$$

The saturation O_2 concentration depends on the O_2 solubility, S_{O_2} [µmol·dm^{-3}·kPa^{-1}],

$$c_{O_2}^{*} = p_{O_2}^{*} \cdot S_{O_2} \quad (11)$$

Oxygen solubility is a function of temperature and composition of the medium. In other words, oxygen solubility, S_{O_2}, is defined as the ratio of partial oxygen pressure and concentration,

$$S_{O_2} = c_{O_2}^{*}/p_{O_2}^{*} \quad (12)$$

D2. Temperature effect on saturation O_2 concentration

$p_{H_2O}^{*}$ (Eq. 10) is the saturation water vapor pressure at experimental temperature. $p_{H_2O}^{*}$ is a function of absolute temperature, T [K], obtained from the experimental temperature, θ, recorded in units °C,

$$T = \theta + 273.15^{*} \quad (13)$$

The saturation water vapor pressure [kPa] is (Table 1),

$$p_{H_2O}^{*} = \exp[(-216961 \cdot T^{-1} - 3840.7) \cdot T^{-1} + 16.4754] \quad (14)$$

Until recently, the atm-standard pressure has been used: 1 atm = 760 mmHg = 101.325 kPa. For pure water in equilibrium with air at this atm-standard pressure, the 'unit standard concentration' of oxygen, C^{*}, is calculated by the polynomial expression,

$$C^{*} = \exp<\{[(-8.621949 \cdot 10^{11} \cdot T^{-1} + 1.243800 \cdot 10^{10}) \cdot T^{-1} - 6.642308 \cdot 10^{7}] \cdot T^{-1} + 1.575701 \cdot 10^{5}\} \cdot T^{-1} - 135.90202> \quad (15)$$

Table 1. Saturation water vapor pressure, $p_{H_2O}^*$, oxygen pressure, $p_{O_2}^*$, and oxygen concentration, $c_{O_2}^*$, at air saturation and standard barometric pressure, p_b^o = 100 kPa, in pure water as a function of temperature. S_{O_2} is the oxygen solubility, independent of choice of standard pressure. f^o is the multiplication factor to convert partial O_2 pressures and concentrations given at atm-standard pressure (1 atm = 101.325 kPa) to the *IUPAC* standard pressure of 100 kPa (compare Eq. 15),

$$f^o = (100-p_{H_2O}^*) / (101.325-p_{H_2O}^*)$$

θ	T	$p_{H_2O}^*$	$p_{O_2}^*$	$c_{O_2}^*$	f^o	S_{O_2}
°C	K	kPa	kPa	µmol·dm^{-3}		µmol·dm^{-3}·kPa^{-1}
40	313.15	7.38	19.40	197.6	0.9859	10.18
37	310.15	6.27	19.63	207.3	0.9861	10.56
35	308.15	5.62	19.77	214.2	0.9862	10.83
30	303.15	4.24	20.06	233.0	0.9864	11.62
25	298.15	3.17	20.28	254.8	0.9865	12.56
20	293.15	2.34	20.46	280.4	0.9866	13.70
15	288.15	1.70	20.59	310.9	0.9867	15.10
10	283.15	1.23	20.69	348.1	0.9868	16.83
5	278.15	0.87	20.76	393.9	0.9868	18.97
4	277.15	0.81	20.78	404.3	0.9868	19.46

D3. Barometric pressure and saturation O_2 concentration

The unit standard concentration and the oxygen concentration at air saturation (Table 1) and actual barometric pressure are related by (compare f^o in Table 1),

$$c_{O_2}^* = C^* \cdot p_{O_2}^*/[(101.325-p_{H_2O}^*)\cdot 0.20946] \cdot F_M$$
$$= C^* \cdot (p_b-p_{H_2O}^*)/(101.325-p_{H_2O}^*) \cdot F_M \quad (16)$$

D4. The barometric altitude relation (BAR)

The partial pressure of oxygen declines with altitude. Hypoxia causes a limitation of maximal aerobic capacity. The V_{O2max} of acclimatized persons declines at high altitude by c. 11% per 1,000 m, whereas the partial oxygen pressure declines by 12% to 14% per 1,000 m up to 6,000 m, and by 15% to 17% per 1,000 m between 6,000 and 9,000 m. The quadratic model atmosphere equation, MAE, was introduced by John B. West to describe the dependence of average barometric pressure and altitude with high accuracy. An exponential function is the basis of the ICAO Standard Atmosphere, which can be fitted to realistic reference data comparable to the MAE. This leads to the barometric altitude relation, BAR, which

expresses the relationship between barometric pressure, p_b, and altitude, h [m], with an even superior fit (Tab. 2):

$$p_b = p_b^\circ \cdot (1 - \frac{0.00616 \cdot h}{288.15})^{5.256} \quad (17)$$

The standard pressure at average sea level, p_b°, is inserted with 101.325 kPa or 760 mmHg to calculate barometric pressure in the respective unit. Compared to the ICAO, only the temperature gradient of -6.5 °C/km (ICAO) was replaced by the parameter -0.00616 °C/m (BAR) which was obtained by a mathematical fit to the reference data in the range of 0 to 9,000 m. 288.15 K is the air temperature of 15 °C at sea level. Deviations between MAE und BAR are less than ±0.06 kPa (0.4 mmHg) in the range of 0 to 9 km altitude. In this context the relevance of mitochondrial oxygen kinetics is discussed briefly. The p_{50} of mitochondrial respiration is 0.01 to 0.1 kPa (0.08 to 0.8 mmHg; this is the partial oxygen pressure at which mitochondrial respiration drops to 50% of maximum values). These generally very low p_{50} values are important for our understanding of some apparently paradoxical mechanisms of muscular acclimatization and adaptation to hypoxia at extreme altitude (Gnaiger 2013).

Table 2. Barometric pressure, p_b, and oxygen partial pressure, p_{O2}, in dry air and respiratory air saturated by water vapor as a function of altitude, h. The decline of respiratory air p_{O2} is expressed relative to sea level or per 1,000 m change of altitude (from Gnaiger 2013).

h [m]	p_b [kPa]	p_b [mmHg]	Dry air $p_{O2,da}$ [kPa]	Respiratory air p_{O2} [kPa]	[mmHg]	Change rel. to sea level	Rel. change p_{O2}/1.000 m
0	101.3	760	21.2	19.9	149		
1,000	90.4	678	18.9	17.6	132	-0.11	-0.12
2,000	80.5	604	16.9	15.6	117	-0.22	-0.13
3,000	71.5	536	15.0	13.7	103	-0.31	-0.13
4,000	63.3	475	13.3	12.0	90	-0.40	-0.13
5,000	55.9	420	11.7	10.4	78	-0.48	-0.14
6,000	49.2	369	10.3	9.0	68	-0.55	-0.14
7,000	43.2	324	9.1	7.7	58	-0.61	-0.15
8,000	37.8	284	7.9	6.6	50	-0.67	-0.16
9,000	33.0	247	6.9	5.6	42	-0.72	-0.17
575 [a]	94.9	712	19.9	18.6	139	-0.07	
1,675 [b]	83.7	627	17.5	16.2	122	-0.19	
4,559 [c]	59.1	443	12.4	11.1	83	-0.44	
5,240 [d]	54.3	407	11.4	10.1	75	-0.50	
5,364 [e]	53.4	401	11.2	9.9	74	-0.50	
8,848 [f]	33.7	252	7.1	5.7	43	-0.71	

a: Innsbruck, A (95.0 kPa; Jul-Aug 2013); ***b***: Schröcken, Körbersee, AT (83.6 kPa; Okt 2013); ***c***: Monte Rosa, IT (58.4 kPa; Aug-Sep 2004); ***d***: Mt Chacaltaya (54.2 kPa; Aug 2012); ***e***: Everst Base Camp (52.7 kPa; Mar 2013); **f**: Mt Everest (12, 13). Numbers in parentheses are measurements of p_b during respirometric studies with the OROBOROS O2k.

D5. O_2 solubility factor in salt solutions

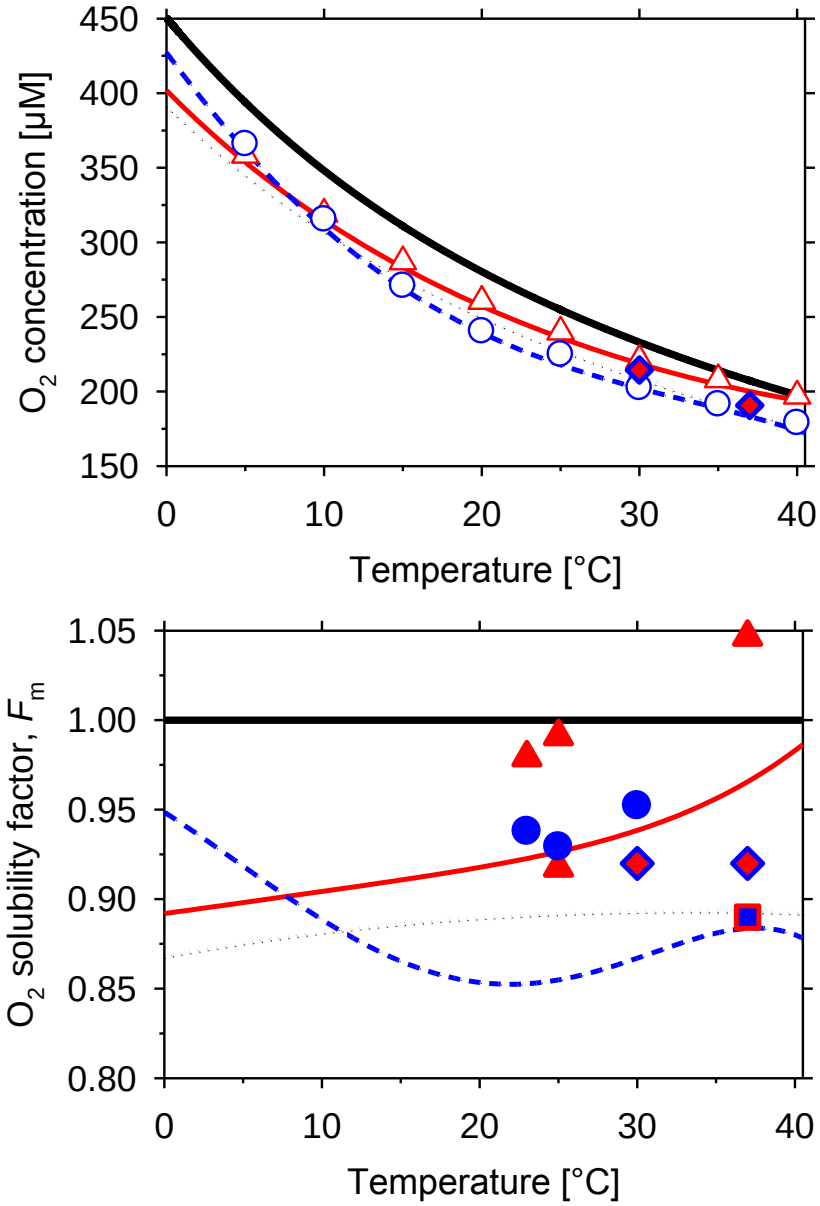

Figure 8. Oxygen concentration at air saturation and standard barometric pressure (100 kPa; top) and oxygen solubility factor (bottom) in MiR05 (diamonds), KCl medium (open trianlges, full line; 150 mmol·dm^{-3} KCl) and sucrose medium (open circles, dashed line; 250 mmol·dm^{-3} sucrose; data for both media from Reynafarje et al 1985), compared to pure water (upper full line) and 20‰ sea water (lower dotted line). For the parameters of the polynomials see Table 2. The solubility factor for serum is shown by the full square (bottom). Literature data (bottom) on KCl media (closed triangles) and sucrose media (closed circles) show (i) the wide scatter of solubility data, (ii) the erroneous use of values even higher than solubility established for pure water, and (iii) a trend to higher values, particularly in sucrose medium, compared to Reynafarje et al 1985 (see References).

The salting out effect is responsible for the reduced oxygen solubility in aqueous solutions compared to pure water (Fig. 8). Detailed equations are available for calculating the oxygen solubility of sea water at different salinities (Forstner and Gnaiger 1983). Physiological solutions commonly used in Oxygraph studies (Rasmussen, Rasmussen 2003; Reynafarje, Costa, Lehninger 1985) are compared with pure water and 20‰ sea water in Fig. 8. The corresponding polynomial equations are summarized in Tab. 3 for calculating the oxygen saturation concentration in equilibrium with air at various temperatures and standard pressure (Tab. 4). Characteristic temperatures are commonly used in experimental studies. Under these conditions it is convenient to use oxygen solubility factors for the medium, F_M (Fig. 8). This factor is independent of barometric pressure, but F_M changes with temperature (compare Fig. 8). The solubility factors are compiled in Tab. 5 for different salinities of sea water (Forstner and Gnaiger 1983) and two typical media used with isolated mitochondria (Reynafarje, Costa,

Lehninger 1985). The latter values have been criticized on methodological grounds by Rasmussen and Rasmussen (2003), and the complex temperature dependence of F_M compared to sea water is doubtful from a thermodynamic perspective Fig. 8).

The oxygen solubility factor of MiR05 (MiR06) is 0.92, at 30 °C and 37 °C (Rasmussen, Rasmussen 2003), corresponding to an oxygen concentration in equilibrium with air under standard conditions ($c_{O_2}^*$) of 214.4 and 190.7 µM, respectively. The oxygen solubility of serum is 9.4 nmol $O_2 \cdot cm^{-3} \cdot kPa^{-1}$ at 37 °C (Baumgärtl and Lübbers 1983). In comparison to the oxygen solubility in pure water (10.56 nmol $O_2 \cdot cm^{-3} \cdot kPa^{-1}$ at 37 °C; Tab. 1), this corresponds to a solubility factor for serum of F_M = 0.89 (Fig. 8) and $c_{O_2}^*$ of 184.5 µM.

Table 3. Parameters of the polynomial fits of oxygen saturation concentration in equilibrium with air at p_b^o = 100 kPa, for sea water (0‰ and 20‰) and typical Oxygraph incubation media, in the range of θ from 5 to 40 °C. Instead of the theoretically based plot of $\ln(S_{O_2})$ versus T^{-1}, the fits were performed on the untransformed data, with temperature, θ, in units of °C ($r^2 \geq 0.999$ in all cases). The equation in nested form is,

$$c_{O_2}^* = \{[(b_4 \cdot \theta + b_3) \cdot \theta + b_2] \cdot \theta + b_1\} \cdot \theta + a$$

Medium	A	B_1	b_2	b_3	b_4
0‰	450.5946	-12.60381	0.2712233	-0.003808	$2.379 \cdot 10^{-5}$
20‰	390.8769	-10.2165	0.2051415	-0.002746	$1.621 \cdot 10^{-5}$
KCl	401.9152	-10.70002	0.2291496	-0.003283	$2.492 \cdot 10^{-5}$
Sucrose	427.411	-14.4983	0.2762108	-0.0003628	$-3.606 \cdot 10^{-5}$

Table 4. Oxygen solubility, S_{O_2} [µM.kPa^{-1}], for seawater at various salinities (10‰, 20‰, 30‰ and 36‰), and for two typical Oxygraph media (concentrations given in mmol·dm^{-3}); "Sucrose": 250 sucrose, 5 KCl, 3 K-Hepes, pH 7.05; "KCl": 150 KCl, 3 K-Hepes, pH 7.05.

θ	S_{O_2} for sea water				S_{O_2} for exp. Medium	
°C	10‰	20‰	30‰	36‰	Sucrose	KCl
40	9.62	9.08	8.58	8.29	8.96	10.01
37	9.98	9.43	8.90	8.61	9.33	10.19
35	10.24	9.67	9.14	8.83	9.54	10.36
30	10.98	10.37	9.80	9.47	10.07	10.90
25	11.86	11.20	10.57	10.21	10.74	11.64
20	12.92	12.19	11.49	11.09	11.70	12.58
15	14.21	13.38	12.59	12.14	13.07	13.75
10	15.79	14.82	13.91	13.39	14.95	15.22
5	17.75	16.60	15.53	14.92	17.42	17.04
4	18.19	17.00	15.89	15.26	17.99	17.45

Table 5. Oxygen solubility factor of the medium, F_M, for seawater at various salinities (10‰, 20‰, 30‰ and 36‰), and for two typical Oxygraph media (concentrations given in mmol·dm^{-3}); "Sucrose": 250 sucrose, 5 KCl, 3 K-Hepes, pH 7.05; "KCl": 150 KCl, 3 K-Hepes, pH 7.05.

θ	F_M for sea water				F_M for exp. Medium	
°C	10‰	20‰	30‰	36‰	Sucrose	KCl
40	0.945	0.892	0.842	0.814	0.880	0.983
37	0.945	0.893	0.843	0.815	0.884	0.966
35	0.945	0.893	0.844	0.815	0.881	0.956
30	0.945	0.893	0.843	0.815	0.867	0.938
25	0.944	0.892	0.842	0.813	0.855	0.926
20	0.943	0.889	0.838	0.809	0.853	0.918
15	0.941	0.886	0.833	0.804	0.865	0.911
10	0.939	0.881	0.827	0.796	0.889	0.904
5	0.936	0.875	0.819	0.786	0.918	0.898
4	0.935	0.881	0.817	0.784	0.925	0.897

References

Baumgärtl H, Lübbers DW (1983) Microaxial needle sensor for polarographic measurement of local O_2 pressure in the cellular range of living tissue. Its construction and properties. In: *Polarographic Oxygen Sensors*, Gnaiger E, Forstner H (eds) Springer, Berlin, Heidelberg, New York:37-65. »

Beavis AD, Lehninger AL (1986) Eur J Biochem 158:315-22.

Brand MD, Harper ME, Taylor HC (1993) Control of the effective P/O ratio of oxidative phosphorylation in liver mitochondria and hepatocytes. Biochem J 291: 739-48.

Chapell JB (1964) Biochem J 90:225-37.

Forstner H, Gnaiger E (1983) Calculation of equilibrium oxygen concentration. In: Polarographic Oxygen Sensors. Aquatic and Physiological Applications. Gnaiger E, Forstner H (eds) Springer, Berlin, Heidelberg, New York:321-33. »

Gnaiger E (2001) Bioenergetics at low oxygen: dependence of respiration and phosphorylation on oxygen and adenosine diphosphate supply. Respir Physiol 128:277-97. »

Gnaiger E (2013) Die barometrische Höhenrelation (BAR): Form und Funktion. Jahrbuch 2013 Österr Ges Alpin- Höhenmed:51-63.

Gnaiger E, Steinlechner-Maran R, Méndez G, Eberl T, Margreiter R (1995) Control of mitochondrial and cellular respiration by oxygen. J Bioenerg Biomembr 27:583-96. »

Hinkle PC, Yu ML (1979) J Biol Chem 254:2450-5.

Lemasters JJ (1984) J Biol Chem 259:13123-30.

Rasmussen HN, Rasmussen UF (2003) Oxygen solubilities of media used in electrochemical respiration measurements. Analyt Biochem 319:105-13.

Rettich TR, Battiono R, Wilhelm E (2000) Solubility of gases in liquids. 22. High-precision determination of Henry's law constants of oxygen in liquid water from T=274 K to T=328 K. J Chem Thermodynam 32:1145-56.

Reynafarje B, Costa LE, Lehninger AL (1985) O_2 solubility in aqueous media determined by a kinetic method. Analyt Biochem 145: 406-18

Stoner CD (1987) J Biol Chem 262:11445-53.

Wilhelm E, Battino R, Wilcock RJ (1977) Low-pressure solubility of gases in liquid water. Chem Rev 77:219-62.